Magnetization and thermal expansion measurements on the Ising magnet $SmPt_2Si_2$: Potential coexistence of spin glass and antiferromagnetic states

Takashi Tayama*
Graduate School of Science and Engineering, University of Toyama, Toyama 930-8555, Japan

Tatsuma D. Matsuda, Ryuji Higashinaka, and Yuji Aoki
Department of Physics, Tokyo Metropolitan University, Hachioji, Tokyo 192-0397, Japan

(Received 29 August 2021; accepted 8 November 2021; published 15 November 2021)

The Ising magnet $SmPt_2Si_2$ undergoes an antiferromagnetic (AFM) transition at $T_{N1} = 5.6$ K, but the magnetic moments of some Sm ions remain disordered even below T_{N1}. Here, we report the results of measurements of thermal expansion, magnetostriction, and dc magnetization of $SmPt_2Si_2$ in the temperature range from 0.26 to 7 K. The magnetization and thermal expansion results show clear irreversible phenomena at temperatures below $T_g \approx 2.4$ K. These results suggest that the partially disordered state of the Sm ions becomes a cluster spin glass below T_g and coexists with the AFM long-range order. However, unlike the conventional coexistence of spin glass and antiferromagnetism, the isothermal magnetization process at 0.26 K shows a hysteresis curve with almost no remanent magnetization. This observation suggests that the cluster spin glass state is an unusual state with a short relaxation time at zero field.

DOI: 10.1103/PhysRevB.104.174418

I. INTRODUCTION

In strongly correlated electron systems, the Ruderman-Kittel-Kasuya-Yosida (RKKY) interaction between the localized magnetic moments of f electrons mediated by conduction electrons and the Kondo effect, which is the shielding effect of the magnetic moment of f electrons by the spin of conduction electrons, may compete with each other. Such competition has set the stage for the study of unconventional superconductivity and quantum critical phenomena, which have been actively studied over the last few decades. The addition of the frustration of magnetic interactions to these interactions raises the interesting question of how the ground state of the system changes [1]. $SmPt_2Si_2$ has received attention as a material that can approach this question [2].

$SmPt_2Si_2$ crystallizes in the tetragonal $CaBe_2Ge_2$-type structure (space group $P4/nmm$). This material is an Ising magnet with the easy axis of magnetization in the c-axis direction and has a large magnetic anisotropy. The magnetic susceptibility in the c-axis direction increases with decreasing temperature according to the Curie-Weiss law, and shows a peak at $T_{N1} = 5.1$ K due to the antiferromagnetic (AFM) transition. In the case of an ordinary Ising AFM order, the susceptibility in the direction of the easy axis of magnetization decreases to zero at absolute zero. However, the observed magnetic susceptibility of $SmPt_2Si_2$ decreases slightly below T_{N1} and then increases again according to the Curie-Weiss law. From analysis of the magnetic susceptibility, Fushiya *et al.* reported that about 70% of Sm ions remain in the paramagnetic state even below T_{N1}. The authors pointed out that this partial disorder may be caused by geometric frustration inherent in the crystalline structure.

The specific heat in zero field shows a rather broad peak at $T^* \approx 1.8$ K in addition to a distinct peak at T_{N1}, but the origin of T^* is not yet clear. Analysis of the specific heat data shows that below T_{N1}, the linear specific heat coefficient $\gamma = C/T$ has a large value of $\gamma = 350$ mJ/mol K^2, and the possibility of a heavy fermion state is discussed. The reported magnetic phase diagram of $SmPt_2Si_2$ when a magnetic field is applied in the c-axis direction consists of a low-field AFM phase I and a high-field AFM phase II; phase I is an AFM state in which the magnetic moments of some Sm ions remain disordered, while phase II is an antiferromagnetically ordered state in which the partially disordered state is resolved. Thus, it has been argued that this compound has three competing interactions: the RKKY interaction, the Kondo effect, and geometric frustration.

The $J = 5/2$ ground state multiplet of Sm^{3+} is sixfold degenerate and splits into three Kramers doublets, $|\pm 1/2\rangle$, $|\pm 3/2\rangle$, and $|\pm 5/2\rangle$, due to the crystalline electric field (CEF) of the tetragonal symmetry. Analysis of the observed susceptibility shows that the ground state of the CEF is a $|\pm 3/2\rangle$ doublet, and that the physical properties at low temperatures are dominated by this $|\pm 3/2\rangle$ doublet. The question is why the partially disordered state arises and what the ground state is, but this is not yet clear because the physical properties below 2 K have hardly been experimentally investigated.

In this paper, we report the results of thermal expansion, magnetostriction, and dc magnetization measurements on a single crystal sample from 0.26 to 7 K in order to clarify the low-temperature properties of the strange AFM phases of $SmPt_2Si_2$, especially the I phase. We observe irreversible phenomena in both magnetization and thermal expansion below

*tayama@sci.u-toyama.ac.jp

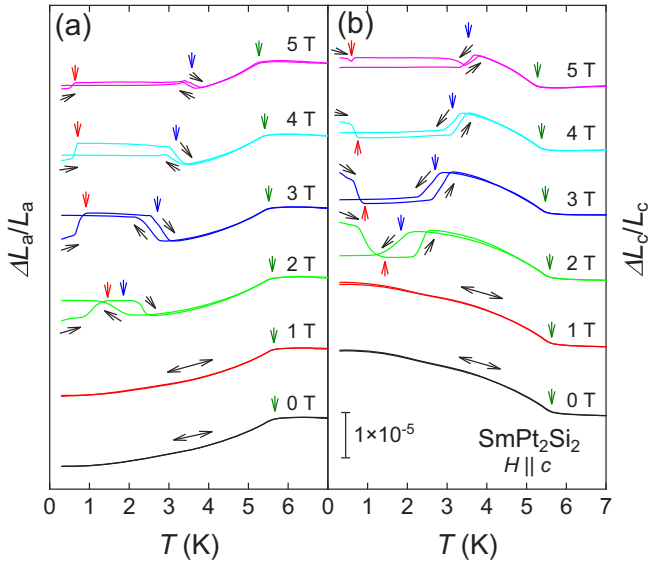

FIG. 1. Temperature dependence of the transverse linear thermal expansion $\Delta L_a(T)/L_a$ (a) and longitudinal linear thermal expansion $\Delta L_c(T)/L_c$ (b) measured in a fixed magnetic field between 0 and 5 T when the magnetic field is applied along the c axis in $SmPt_2Si_2$. Each data was taken with increasing temperature after ZFC, and then with decreasing temperature. The green arrow indicates the AFM transition temperature T_{N1}, the blue arrow indicates the magnetic structure transition temperature T_{N2}, and the red arrow indicates the temperature T_g (see text). Note that the two panels are on the same scale.

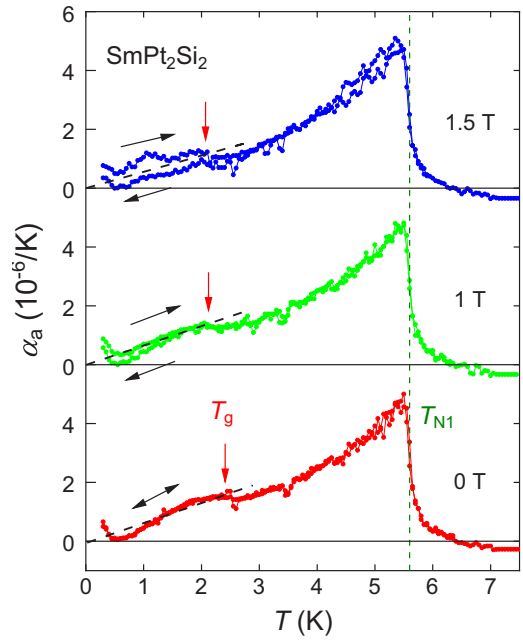

FIG. 2. Temperature dependence of the transverse linear thermal expansion coefficient α_a measured at magnetic fields of 0, 1, and 1.5 T in $SmPt_2Si_2$. The red arrow indicates the onset temperature of the broad peak, T_g. The black dashed line is a straight line fitting through the origin for data below T_g. The green dashed line indicates T_{N1}.

$T_g \approx 2.4$ K. These results suggest that the partially disordered state becomes a cluster spin glass state below T_g and coexists with the AFM order. Unlike ordinary spin glasses, however, the isothermal magnetization process at 0.26 K shows a hysteresis curve, but the remanent magnetization is negligibly small. These observations imply that the cluster spin glass of phase III is a unique state with a short relaxation time in zero field.

II. EXPERIMENTAL

Single crystal samples of $SmPt_2Si_2$ were grown by the Sn flux method. The details of the single crystal samples are described in Ref. [2]. The mass of the sample used in this study is only 1.13 mg, and the length along the a axis of the sample is $L_a = 0.73$ mm, and the length along the c axis is $L_c = 0.29$ mm. Thermal expansion and magnetostriction measurements were carried out using the capacitance method. The capacitive dilatometer used here allows one to measure samples of any shape and has a high resolution of 0.01 Å to 0.1 Å. Only one side of the sample was fixed to the sample stand of the dilatometer with varnish, and the other side was in contact with the movable electrode plate of the parallel plate condenser. In this paper, the volume thermal expansion $\Delta V/V$ is calculated using the equation $\Delta V/V = 2\Delta L_a/L_a + \Delta L_c/L_c$, assuming the tetragonal structure regardless of temperature and magnetic field.

The dc magnetization measurements were performed using the capacitive Faraday method [3]. The sensitivity of the magnetometer is about $10^{-6} \sim 10^{-5}$ emu, and the background magnetic susceptibility χ_{bg} is as small as -2×10^{-9} emu. In this measurement, a magnetic field gradient of 5 T/m was used. The capacitance readings in the thermal expansion and magnetization measurements were taken using a high-sensitivity capacitance bridge (Andeen-Hagerling, model 2500A).

The sample was mounted on a ^{3}He refrigerator. The magnetic field was always applied along the c axis of the tetragonal crystal in both thermal expansion and magnetization measurements. The longitudinal ($H \parallel L$) and transverse ($H \perp L$) magnetostrictions were measured using a solenoidal superconducting magnet and a split-pair superconducting magnet, respectively. The temperature range of the measurements was 0.26–7 K, and the magnetic field range was 0–5 T. As we will see later, the magnetic state of $SmPt_2Si_2$ is irreversible at low temperatures. Thus, all data in this paper were subjected to zero-field cooling (ZFC) from temperatures above T_{N1} before measurement.

III. RESULTS

A. Thermal expansion and magnetostriction

Figure 1(a) shows the magnetic field variation of the transverse linear thermal expansion $\Delta L_a(T)/L_a$ versus temperature up to 5 T in $SmPt_2Si_2$. Each data was taken with increasing temperature after ZFC, and then with decreasing temperature. The data at zero field show a clear bend at $T_{N1} = 5.6$ K, which is due to the AFM transition. This value of T_{N1} is slightly higher than the previously reported value ($T_{N1} = 5.1$ K). We believe that this difference in T_{N1} is due to sample dependency.

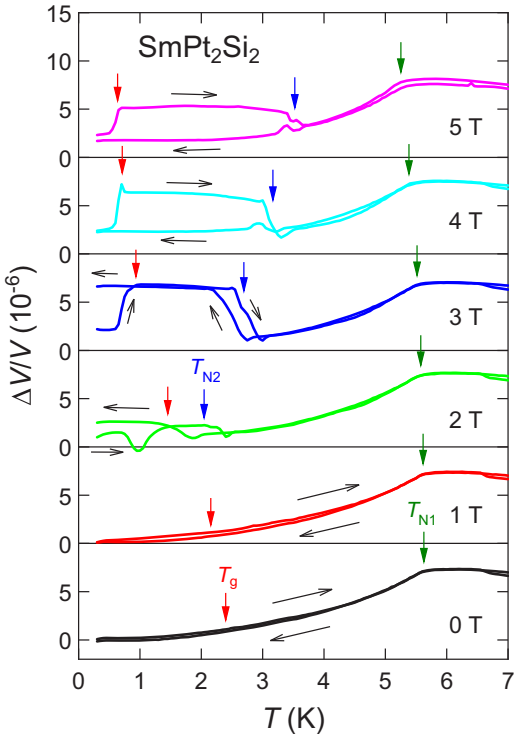

FIG. 3. Temperature dependence of volume thermal expansion determined from experimental results of linear thermal expansion of $SmPt_2Si_2$. The green arrow indicates T_{N1}, the blue arrow indicates T_{N2}, and the red arrow indicates T_g.

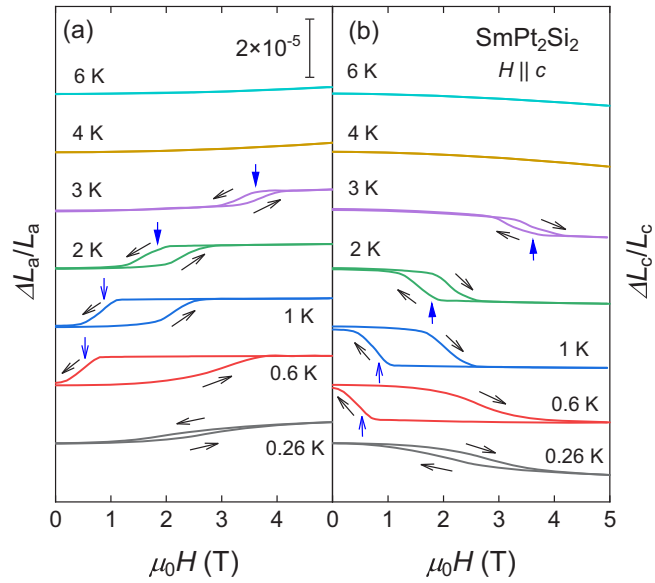

FIG. 4. Magnetic field dependence of the longitudinal (a) and transverse (b) magnetostrictions of $SmPt_2Si_2$ measured at selected temperatures between 0.26 K and 6 K. The blue arrow shows the transition field from phase II when the magnetic field is reduced (see text). Note that the two panels are on the same scale.

The data at 0 T show no noticeable anomalies below T_{N1}, and the data at 1 T are almost identical to those at zero field. However, the results at 2 T are qualitatively different, showing a length discontinuity with hysteresis at $T_{N2} = 2$ K, and a significant difference between ZFC and field cooling (FC) below $T_g = 1.4$ K. Here we take T_{N2} as the average value of the peak temperature of the linear expansion coefficient during the heating and cooling process (not shown), and T_g as the onset temperature of the hysteresis (T_g can be more clearly defined by the magnetization data shown later). The anomaly at T_{N2} is due to a first-order transition between phase I and phase II. As the magnetic field is further increased, the values of T_{N1} and T_g gradually decrease, while the value of T_{N2} increases significantly. This magnetic field dependence of T_{N1} and T_{N2} is reasonably consistent with previous reports [2]. Likewise, the magnetic field variation of longitudinal thermal expansion $\Delta L_c(T)/L_c$ vs temperature is plotted in Fig. 1(b). The result of longitudinal linear thermal expansion is almost exactly opposite to that of transverse linear thermal expansion. This is a common behavior to reduce the volume change, since volume change is generally accompanied by a large energy change.

To confirm the results of the transverse linear thermal expansion at magnetic fields lower than 2 T in more detail, the temperature dependence of the transverse linear thermal expansion coefficient $\alpha = d(\Delta L/L)/dT$ is plotted in Fig. 2. In addition to a sharp jump at T_{N1}, the 0 T data shows a very broad peak around 2.4 K. This peak is quite similar to the peak at $T^* \approx 2$ K reported for zero-field specific heat [2]. Therefore, the origin of these peaks is most likely the same. As the magnetic field is increased, the position of the peak shifts slightly to a lower temperature. Furthermore, below the onset temperature of this peak, temperature hysteresis gradually develops as the magnetic field increases. As we will see later from the magnetization results, the onset temperature of this peak is of the same origin as the onset temperature T_g of the irreversible phenomenon above 2 T. So, we define T_g as the onset temperature of this peak. As shown by the red dashed line in the figure, the $\alpha(T)$ data below T_g is almost proportional to the temperature. Note that the $\alpha(T)$ data has an upturn below 0.5 K. A similar behavior was observed for specific heat, which was reported to be due to the nuclear magnetic moment of Sm [2]. However, the upturn in the thermal expansion coefficient was almost independent of the magnetic field, so it is unclear whether it is due to the nuclear moment of Sm.

Figure 3 shows the volume thermal expansion obtained from the results of longitudinal and transverse linear thermal expansions. Since the volume shrinks when the transition from paramagnetic phase to phase I occurs at T_{N1}, T_{N1} should increase when hydrostatic pressure is applied. On the contrary, the volume expands at T_{N2}, so T_{N2} should decrease with hydrostatic pressure. Note that these data, especially those below T_{N2}, have not changed systematically. This is probably due to slightly different conditions such as temperature when measuring longitudinal and transverse linear thermal expansion, and is not an intrinsic behavior.

Figures 4(a) and 4(b) show the results of longitudinal and transverse magnetostriction of $SmPt_2Si_2$. The behavior of longitudinal magnetostriction and transverse magnetostriction is opposite, with longitudinal magnetostriction shrinking and transverse magnetostriction stretching as the magnetic field

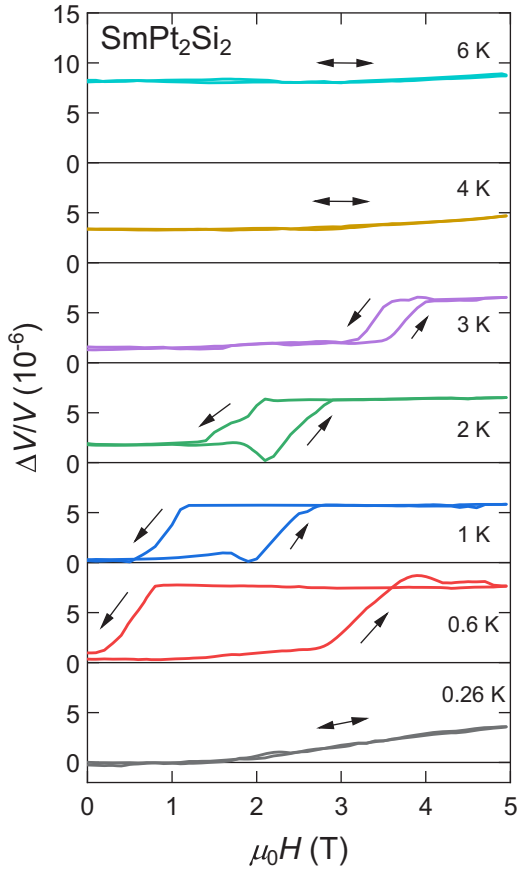

FIG. 5. Magnetic field dependence of the volume magnetostriction $\Delta V(H)/V$ obtained from linear magnetostriction in $SmPt_2Si_2$.

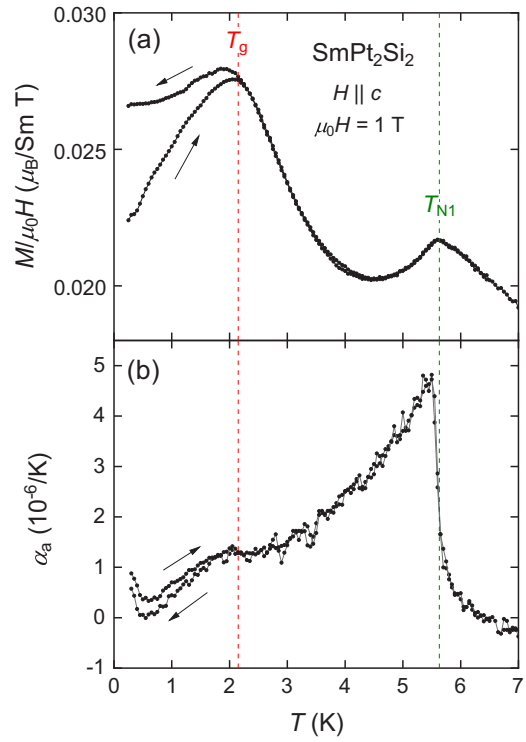

FIG. 6. Temperature dependence of dc magnetization $M(T)/\mu_0 H$ (a) and linear transverse thermal expansion coefficient $\alpha(T)$ (b) of $SmPt_2Si_2$ when a magnetic field of 1 T is applied along the c axis. T_g is the temperature at which irreversibility develops. The dashed lines are guides for the eyes.

increases. The 6 and 4 K data changes smoothly, with no distinct anomalies. On the other hand, the 3 K data shows a jump with hysteresis around 3.5 T (indicated by blue arrow). Note that the blue arrows above 2 K are the average magnetic fields of the peaks in the field derivatives of the magnetization and demagnetization processes, and the blue arrows below 1 K are the magnetic fields of the peaks in the field derivatives of the demagnetization process. This is due to the first-order phase transition from phase I to phase II. As the temperature is lowered further, the first-order phase transition field moves to lower fields, and the width of the hysteresis increases. Also note that there is a small but finite residual magnetostriction in the 0.6 and 1 K data. In contrast, the data at 0.26 K shows a hysteresis curve, but no first-order phase transition. This indicates a large change in the magnetic state between 0.6 and 0.26 K.

Figure 5 shows the volume magnetostriction obtained from the linear magnetostriction results. It can be seen that the volume expands in the transition from phase I to phase II. At 0.26 K, the linear magnetostriction has hysteresis, but the volume magnetostriction has no hysteresis. This is because the hysteresis of longitudinal magnetostriction and transverse magnetostriction just cancel each other out. Note that the somewhat unnatural results are probably due to slight differences in the measurement conditions for longitudinal and transverse magnetostriction.

B. dc magnetization

Figure 6(a) shows the temperature dependence of the dc magnetization $M(T)/H$ of $SmPt_2Si_2$ when a magnetic field of 1 T is applied along the c axis. For comparison, the result of the linear transverse thermal expansion coefficient $\alpha(T)$ at 1 T is also plotted in Fig. 6(b). The two data were taken by increasing the temperature to 7 K after ZFC, and then decreasing the temperature. The M/H curve peaks at $T_{N1} = 5.6$ K and increases again below T_{N1} according to the Curie-Weiss law. This behavior is the same as in the previous report. However, as the temperature decreases further, the M/H data gradually deviates from the Curie-Weiss law and shows a peak. There is also a clear difference between the ZFC and FC data below $T_g \approx 2.4$ K. The $\alpha(T)$ data, on the other hand, shows a broad peak and weak but irreversibility below T_g. Therefore, the onset temperature of the broad peak in $\alpha(T)$ can be regarded as the same as T_g. The temperature dependence of the magnetization M/H measured at several fixed magnetic fields up to 5 T is shown in Fig. 7. The data above 2 T show a first-order transition with hysteresis at T_{N2}, in addition to anomalies at T_{N1} and T_g. These results are consistent with the thermal expansion results in Fig. 1.

Figure 8 shows the isothermal magnetization process measured at temperatures from 0.26 to 6 K after ZFC. The 6 K data shows no clear anomaly, but the 3 K data shows a magnetization jump due to the first-order transition at around 3.3 T. As the temperature decreases, this first-order transition field moves to lower fields, and the hysteresis curve becomes larger.

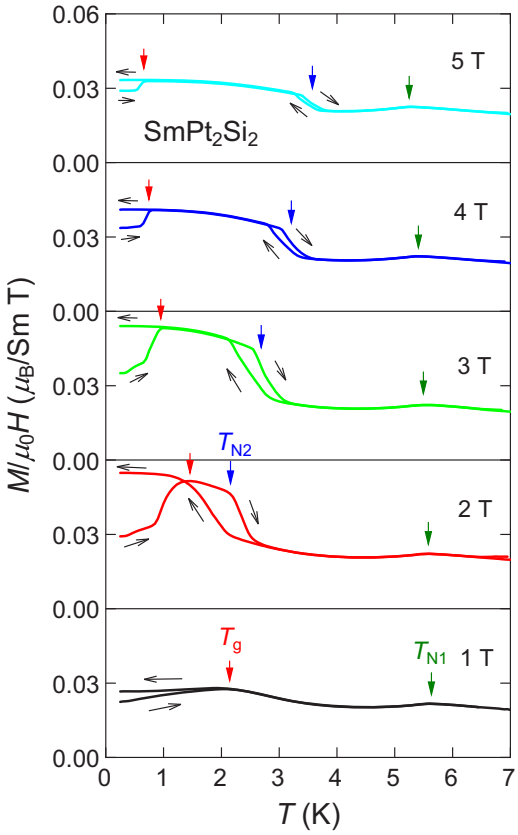

FIG. 7. Temperature dependence of the magnetization $M(T)/H$ of $SmPt_2Si_2$ measured at several fixed magnetic fields between 1 T and 5 T. The green arrow indicates T_{N1}, the blue arrow indicates T_{N2}, and the red arrow indicates T_g.

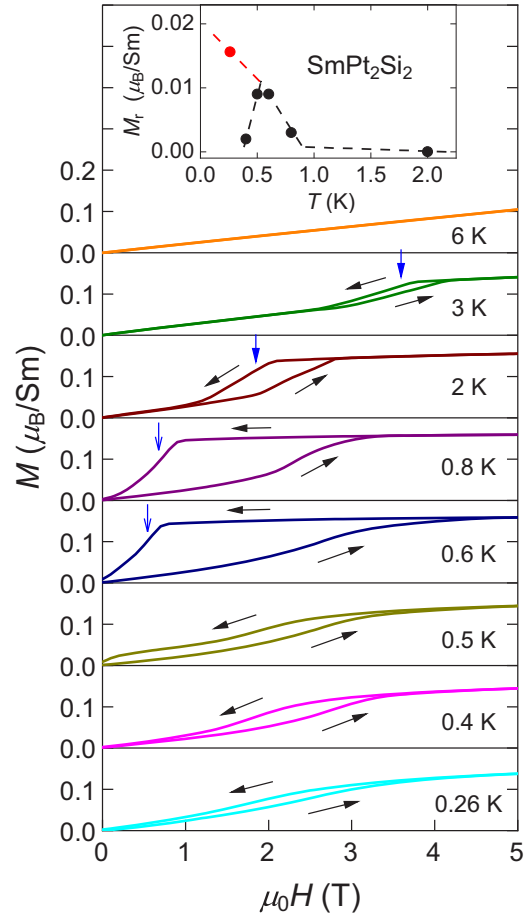

FIG. 8. Isothermal magnetization curve $M(H)$ of $SmPt_2Si_2$ measured at selected temperatures between 0.26 and 6 K. All results were taken after ZFC. The blue arrow shows the transition field from phase II when the magnetic field is reduced. Inset: temperature dependence of the remanent magnetization $M_r(T)$ obtained from the measurement of the $M(H)$ process (black circles). The red circle indicates the remanent magnetization when the $M(H)$ process is measured through phase II. See the text for details. The dashed lines are guides for the eyes.

The data at 0.6 K also shows a distinct remanent magnetization. However, the result at 0.5 K is entirely different from the result at 0.6 K. The first-order transition disappears and the hysteresis curve becomes sharply smaller. If we carefully compare the results for 0.6 K and 0.5 K, we can see that the results for increasing the magnetic field are almost the same, but the results for decreasing the field are significantly different. This means that the difference between the 0.6 and 0.5 K data is due to the presence or absence of magnetization jump when the magnetic field is decreased. Interestingly, the remanent magnetization disappears in the data below 0.4 K. We summarize the temperature variation of the obtained remanent magnetization $M_r(T)$ in the inset of Fig. 8. The $M_r(T)$ value increases with decreasing temperature below 1 K, away from T_g, and reaches a maximum around 0.5 K, and then decreases rapidly. This result also suggests an abrupt change in the magnetic state below 0.5 K.

Figure 9 shows the H–T phase diagram of $SmPt_2Si_2$ for $H \parallel c$ as determined from the present thermal expansion, magnetostriction, and dc magnetization measurements. The filled circles represent the second-order phase transition temperature T_{N1} from the paramagnetic phase to phase I, and the open circles represent the first-order phase transition temperature T_{N2} from phase I to phase II. T_{N2} is defined as the average of the peak temperatures during the heating and cooling processes of the differential magnetization $dM(T)/dT$ or the thermal expansion coefficient $\alpha(T)$. The filled squares represent the onset temperature T_g, at which irreversibility appears, and the region below T_g is designated as phase III. The cross symbols represent the magnetic field of the II-III phase transition observed when the field is decreased in the $M(H)$ and $\Delta L(H)/L$ data. Phase I is an AFM phase with a partially disordered state, while phase II is probably a state in which all magnetic moments are antiferromagnetically ordered. When compared to previous magnetic phase diagrams, which were only reported in the temperature range above 2 K, the results are in close agreement, except that the T_{N1} values are slightly higher than in the past [2]. The present magnetic phase diagram further reveals the presence of phase III. Compared to the phase boundary between phases I and III, the phase boundary between phases II and III appears to be pushed to the lower temperature side. In addition, the slope of the phase boundary of phase III appears to diverge toward absolute zero. Below 0.5 K (light gray region), the

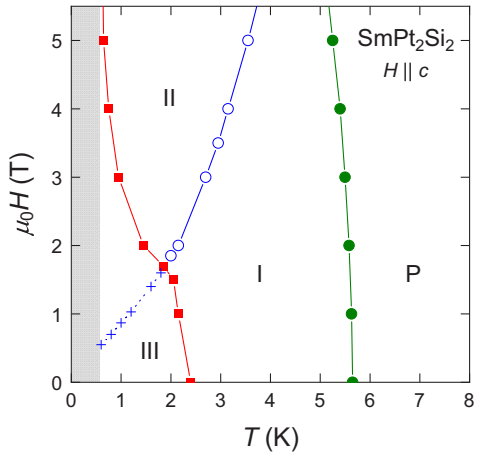

FIG. 9. H–T phase diagram of $SmPt_2Si_2$ for $H \parallel c$ as determined from the present measurements. The green closed (T_{N1}), blue open (T_{N2}) circles and red squares (T_g) are the transition point obtained from Figs. 1, 2, and 7. The cross symbols are the one obtained from Figs. 4 and 8. Phase P is the paramagnetic phase. Phase I is an AFM phase with a partially disordered state. Phase II is an AFM phase with no partially disordered state. Phase III is a coexisting phase of spin glass and antiferromagnetism. Below 0.5 K (light gray region), the II-III phase transition disappears.

first-order transition from phase III to phase II and remanent magnetization are not observed.

Let us now consider why the remanent magnetization disappears in the isothermal magnetization process below 0.5 K. This might be related to the fact that the II-III phase transition does not exist below 0.5 K. In order to confirm this, the following measurements were carried out; starting with phase II at 5 T and 2 K and then lowering the temperature of the sample to 0.26 K. The magnetization data was then acquired with decreasing the magnetic field from 5 to 0 T. The result (red dots) is shown in Fig. 10, which is completely different from the result measured by the usual procedure (black dots);

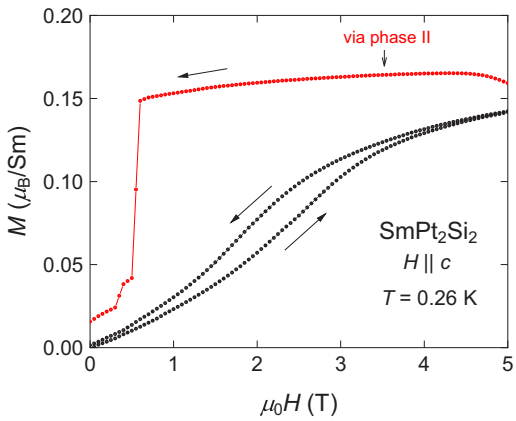

FIG. 10. Isothermal magnetization process of $SmPt_2Si_2$ at 0.26 K. The black line is the result of measurement in the normal procedure. The red line is the result obtained by the following procedure; we started with the state in phase II above 2 K at 5 T, and then lowered the temperature to 0.26 K. The data was then taken with decreasing the field from 5 T to 0 T.

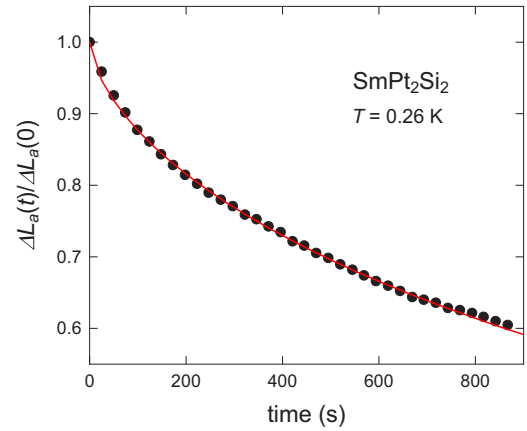

FIG. 11. Time variation of the remanent magnetostriction ratio $\Delta L_a(t)/\Delta L_a(0)$ in zero field immediately after magnetostriction measurement at 0.26 K after going through phase II. The red line is the result of fitting the data with the stretched exponential relaxation function $\exp(-(t/\tau)^{\beta})$. The relaxation time $\tau = 2500$ s and the stretching exponent $\beta = 0.63$ are obtained.

the red data shows a sharp magnetization jump of about 0.1 μ_B/Sm at 0.5 T and a large remanent magnetization. We plot the obtained remanent magnetization values (red dot) in the inset of Fig. 8, and see that the remanent magnetization monotonically increases with decreasing temperature. Thus this proves that the remanent magnetization appears only when the II-III phase transition occurs.

The saturation value in the $M(H)$ curve at 0.26 K is about 0.15 μ_B/Sm, which is one third of the full moment of the $|\pm 3/2\rangle$ doublet, 0.45 μ_B/Sm. Hence, an up-up-down magnetic structure has been proposed for phase II [2]. However, when the isothermal magnetization process is measured at 0.26 K through phase II (red line), the saturation value of magnetization exceeds 0.15 μ_B/Sm, suggesting that phase II may be a more complex magnetic structure. Note that in the red data in Fig. 10, the magnetization increases even though the magnetic field is reduced from 5 to $\sim$ 4.5 T. The reason for this is probably that the magnetization is in the process of relaxing in the direction of increasing.

We also investigate the time variation of the residual magnetostriction by magnetostriction measurement. The obtained result (Fig. 11) shows a distinct relaxation phenomenon. Fitting the data with the stretched exponential relaxation function $\exp(-(t/\tau)^{\beta})$ yields the relaxation time $\tau = 2500$ s and the stretching exponent $\beta = 0.63$. The stretched exponential relaxation is known to be compatible with many relaxation processes in disordered and quenched electron and molecular systems, and the value of β obtained is close to the magic number $\beta = 3/5$ for short-range forces [4]. In addition, the τ value is rather short, suggesting that the magnetic moments are not completely frozen even at 0.26 K.

IV. DISCUSSION

A. Partially disordered state in phase I

First, we consider the partially disordered state of phase I of $SmPt_2Si_2$. According to a previous report, about 70%

TABLE I. Parameters of CEF interaction and magnetic molecular field coefficients.

B_2^0(K)	B_4^0(K)	$B_4^4(K)$	n_1(T/μ_B)	n_2(T/μ_B)
8	1	0	−21.8	21.2

of Sm ions remain in the paramagnetic state in phase I [2]. However, this evaluation ignores the AFM susceptibility below T_{N1}, which is probably overestimated in this ratio. Thus, we try to calculate the AFM susceptibility below T_{N1} using the mean-field approximation. Unfortunately, we do not know the magnetic structure of phase I at present, so we assume an AFM structure with two sublattices (A, B) and introduce the following Hamiltonian:

$$\mathcal{H}_{A(B)} = \mathcal{H}_{CEF} - g_J\mu_B \boldsymbol{J}\cdot(\boldsymbol{H} + n_1\langle\boldsymbol{M}\rangle_{B(A)} + n_2\langle\boldsymbol{M}\rangle_{A(B)}). \tag{1}$$

Here $\mathcal{H}_{CEF}$ is the CEF Hamiltonian for the subspace of $J = 5/2$ multiplet and can be expressed as follows:

$$\mathcal{H}_{CEF} = B_2^0 O_2^0 + B_4^0 O_4^0 + B_4^4 O_4^4, \tag{2}$$

where O_i^j and B_i^j are the Stevens operators and the CEF parameters, respectively. The values of the CEF parameters are not yet known. Therefore, we determine the value of B_i^j to fit the experimental results of the magnetic susceptibility in the paramagnetic state as well as possible. The obtained values of B_i^j are summarized in Table I. The CEF levels obtained (see Table II) are $|\pm 3/2\rangle$ for the CEF ground state, $|\pm 1/2\rangle$ for the first excited state at 252 K, and $|\pm 5/2\rangle$ for the second excited state at 336 K.

The second term in Eq. (1) is the Zeeman Hamiltonian, and the third and fourth terms are the first and second nearest neighbor magnetic interaction Hamiltonians of the Heisenberg type in the mean-field approximation. n_1 and n_2 are the molecular field coefficient parameters. According to Ref. [2], the paramagnetic Curie temperature θ_P is as small as θ_P=−0.46 K, even though T_{N1} is 5.1 K. To reproduce these experimental values, we have taken into account the magnetic interactions up to the second nearest neighbor. The obtained values of the molecular field coefficient parameters are also summarized in Table I.

The magnetic susceptibility χ_{AFM} calculated based on the two sublattice model using the mean-field approximation is shown in Fig. 12(a), where χ_P is the result for the one sublattice model. The calculations in the paramagnetic state reproduce the experimental results quite well, including the magnetic anisotropy. Below T_{N1}, χ_{AFM} in the c-axis direction gradually decreases and becomes zero at absolute zero. Then,

TABLE II. Energy levels, representation and wave functions.

Energy (K)	Representation	Wave functions
0	$\Gamma_7^{(1)}$	$\|\pm 3/2\rangle$
252	Γ_6	$\|\pm 1/2\rangle$
336	$\Gamma_7^{(2)}$	$\|\pm 5/2\rangle$

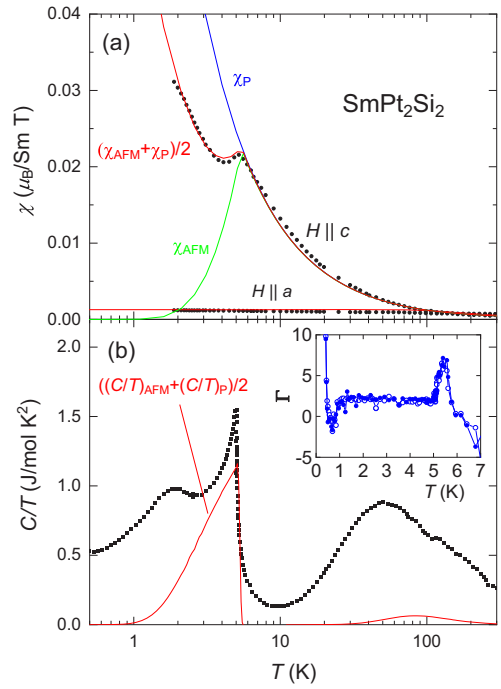

FIG. 12. (a) Calculated results of magnetic susceptibility χ of $SmPt_2Si_2$. The green and blue lines are the results calculated with the two- and one sublattice models, respectively. The red line is their average. (b) Calculated result of zero-field specific heat C/T. Note that the model does not include contributions from partially disordered states and phonons. The black dots in both (a) and (b) are experimental results from Ref. [2]. Inset: temperature dependence of the Grüneisen parameter in $SmPt_2Si_2$ in zero magnetic field. The specific heat data are taken from Ref. [2]. The bulk modulus B_T used in the evaluation is 100 GPa and the molar volume V_m is 5.21×10^{-5}m^3/mol. The filled and open circles are the result on heating and cooling, respectively.

if we take the average of χ_{AFM} and χ_P, we get the red line in the figure. Interestingly, the red line agrees well with the experimental results below T_{N1}. Hence, in this model, the percentage of disordered states below T_{N1} is 50%. We also show the results of the specific heat calculation in Fig. 12(b). The sharp peak at 5.2 K and the small peak around 100 K are due to the AFM transition and the CEF excited states, respectively. Note that the height of the peak at T_{N1} in the calculation result (red line) is half of the value when the magnetic moments of all Sm ions are involved in the AFM transition. Since the model does not include partially disordered states or contributions from phonons, this calculation result is probably reasonable.

B. Frustration of magnetic interactions in phase I

Here we consider frustration, which is a possible cause of the partial disorder state in phase I. In general, there are two types of frustration in magnetic interactions: geometrical frustration resulting from the geometrical situation of one type of magnetic interaction, and magnetic frustration due to the competition between several types of magnetic interactions. We first discuss the possibility of geometrical frustration in $SmPt_2Si_2$. The strength of geometric frustration

is usually measured by the index $f = |\theta_P|/T_m$, where θ_P is the paramagnetic Curie temperature and T_m is the magnetic transition temperature. For systems with strong geometric frustration, the value of f is larger than ten. For example, the Kagome lattice antiferromagnet $SrCr_8Ga_4O_{19}$, known as a strongly geometrically frustrated system, has $f = 150$ [5]. In the case of $SmPt_2Si_2$, the values of θ_P=−0.46 K and $T_m = 5.1$ K give $f = 0.08$, indicating that the geometric frustration effect is small. Therefore, we conclude that the possible frustration in $SmPt_2Si_2$ is magnetic frustration due to the competition between several types of magnetic interactions.

According to the previous discussion in subsection A, the nearest neighbor magnetic interaction J_1 is AFM ($J_1 < 0$) and the second nearest neighbor magnetic interaction J_2 is ferromagnetic ($J_2 > 0$). Based on the crystalline structure of $SmPt_2Si_2$, J_1 is the nearest neighbor interaction in the c plane and J_2 is the nearest neighbor interaction between the c planes. In this case, the magnetic moment of the system is frustrated, and this might be the cause of the partial disorder.

C. Summary of experimental results in phase III

Next, we will discuss phase III. This experiment has revealed the following characteristics of phase III:

(1) The coefficient of linear thermal expansion $\alpha(T)$ in zero field has a broad peak at $T_g \approx 2.4$ K, as does the specific heat, and is highly proportional to temperature below T_g.

(2) The temperature dependence of $M(T)/H$ shows a large difference between the ZFC and FC results below T_g.

(3) The isothermal $M(H)$ process below T_g shows a hysteresis curve.

(4) The slope of the phase III boundary line in the H–T phase diagram is divergent toward absolute zero.

(5) When the II-III phase transition is allowed to occur, the isothermal $M(H)$ curve has a large remanent magnetization, and the value of the remanent magnetization increases as the temperature decreases.

(6) At temperatures below 0.5 K, the first-order transition between phases II and III disappears, and the remanent magnetization is negligibly small.

D. Heavy fermion state in phase III

First, let us consider the result of No. 1. The analysis of the specific heat below T_{N1} gives an enhanced linear specific heat coefficient of $\gamma = 350$ mJ/mol K^2, and the existence of heavy fermion states has been argued. However, it is known that the specific heat is proportional to the temperature at low temperatures even in quantum spin liquid and spin glass states. Thus it is also important to examine other physical quantities to confirm that the system is a heavy fermion system. In heavy fermion systems, not only is the electronic specific heat coefficient γ large, but the electronic Grüneisen parameter Γ is also large. For example, the typical heavy fermion compound $CeRu_2Si_2$ has $\gamma = 350$ mJ/mol K^2 and $\Gamma = 175$ [6]. In the case of normal metals, both γ and Γ are roughly in the order of one order of magnitude. Therefore, we evaluate the value of the electronic Grüneisen parameter of $SmPt_2Si_2$. The Grüneisen constant Γ is defined by the relation $\Gamma = V_m B_T \beta/C$, where V_m is the molar volume and B_T is the bulk modulus. Since the bulk modulus B_T of $SmPt_2Si_2$ has not yet been measured, we use the same value as $B_T = 100$ GPa for $CePt_2Si_2$, which is isostructural to $SmPt_2Si_2$ [7]. The specific heat C used in the calculation is taken from Ref. [2]. The Grüneisen parameter of $SmPt_2Si_2$ derived in this way is shown in the inset of Fig. 12(b). A peak around T_{N1} in the figure is due to the difference in T_{N1} of the samples used for the measurement of specific heat ($T_{N1} = 5.1$ K) and volume thermal expansion ($T_{N1} = 5.6$ K). So if we ignore the result above 5 K, the value of Γ is roughly 2. This value of Γ includes magnetic and phonon contributions, but the temperature is sufficiently low that Γ can be regarded as an electronic Grüneisen constant. Hence, we can conclude that the origin of the large value of C/T is probably not due to the electronic specific heat coefficient, but to the quantum spin liquid or spin glass. Note that Γ shows a sharp increase below 0.5 K. The cause of this is not known at present.

E. Quantum spin liquid in phase III

We consider the possibility of a quantum spin liquid in the III phase of $SmPt_2Si_2$. Quantum spin liquids are expected to exhibit liquidlike behavior characterized by a specific heat proportional to temperature, a magnetic susceptibility that follows the Curie law, and a nearly linear magnetization curve at low magnetic fields [8]. In $SmPt_2Si_2$, the zero-field specific heat is proportional to the temperature at low temperatures. However, below T_{N1}, the magnetic susceptibility increases according to the Curie-Weiss law, not the Curie law, and below T_g, the magnetic susceptibility changes irreversibly. The magnetization process at 0.26 K is nearly linear at low fields, but has field hysteresis. Furthermore, the CEF ground state is $|\pm 3/2\rangle$, and its quantum fluctuation seems to be smaller than that of quantum spin liquids with spin-1/2. Therefore, it is unlikely that phase III is a quantum spin liquid.

F. Spin glass in phase III

The results of No. 1–5 are almost consistent with the features of spin glass, so it is highly likely that there is a spin glass state in phase III. Furthermore, this spin glass is probably a cluster spin glass, as it originates from a partially disordered state. Therefore, we conclude that the cluster spin glass and the long-range AFM order coexists in phase III. Then we consider the result of No. 6. As experimentally demonstrated, the abrupt decrease in remanent magnetization below 0.5 K (Fig. 8) is attributed to the disappearance of the II-III phase transition. So the absence of remanent magnetization is a characteristic of phase III. This indicates that the magnetic moment is not fully frozen at zero field in phase III, which is clearly different from the conventional spin glass order. We believe that this is due to the small size of the cluster spin glass.

Let us now consider the origin of the spin glass in $SmPt_2Si_2$. Typical spin glass materials include CuMn and AuFe, which are alloys of nonferromagnetic metals with a small number of magnetic atoms added to them [9]. The elemental substitution systems of $Fe_xMn_{1-x}TiO_3$ [10] and $Fe_{0.55}Mg_{0.45}Cl_2$ [11] are well known as spin glass compounds. Spin glasses require randomness and frustration in magnetic

interactions, and it is obvious that all of the above materials have randomness due to disorder in the crystal lattice. However, it is not obvious whether $SmPt_2Si_2$ has randomness or not. An example of a material with nontrivial randomness is the semiconductor Sm_3Te_4 [12]. This material is a mixed-valence compound in which Sm^{3+} and Sm^{2+} ions are spatially randomly distributed, and this causes a spin-glass transition to occur at low temperatures. $SmPt_2Si_2$ should have either a disordered crystal lattice or non-trivial randomness. We mention here that the value of the residual resistivity ratio of this material is only 2.3 and the sample dependence of T_{N1} is large [2]. In contrast, the residual resistance ratio of $SmIr_2Si_2$ (but of the tetragonal $ThCr_2Si_2$ type) grown by the same Sn flux method is as large as 270 [13]. These facts may suggest that some imperfection in the crystal of $SmPt_2Si_2$ induces the spin glass state. However, preliminary results show that the T_g values are higher for samples with larger RRR [14]. This implies that the phase diagram obtained in this study is intrinsic. Consequently, the origin of the randomness is unknown at present and will be a subject for future work.

Finally, a comparison with other systems in which spin glass and antiferromagnetism coexist will be made. $Fe_{0.55}Mg_{0.45}Cl_2$ exhibits an AFM transition followed by a spin glass transition, resulting in a coexistence of AFM and spin glass states [11]. $CeNi_2Sn_2$ undergoes a spin-glass transition at around 5 K followed by an AFM transition at 2 K [15]. In the spin glass state of these materials, the magnetic moments are well frozen. On the other hand, in phase III of $SmPt_2Si_2$, the magnetic moments do not seem to be completely frozen at zero field. In this respect, $SmPt_2Si_2$ is an unusual material for a system in which spin glass and antiferromagnetism may coexist. On the other hand, recent neutron scattering experiments on $SmPt_2Si_2$ have reported the absence of magnetic Bragg reflections at 0.3 K [16], and therefore it is not clear whether the spin glass state and the AFM state coexist in phase III. Thus, further experimental studies are needed to clarify phase III.

V. SUMMARY

In this paper, thermal expansion, magnetostriction, and magnetization measurements were performed to clarify the state of the AFM phase with a partially disordered state in Ising magnet $SmPt_2Si_2$. We found that the linear thermal expansion coefficient in zero field has a broad peak at $T_g \approx 2.4$ K, as does the specific heat. Significantly, the temperature dependence of the magnetization at 1 T deviates from the Curie-Weiss law below T_g, and a difference appears between the ZFC and FC results. These results suggest that the magnetic moment in a partially disordered state forms a cluster spin glass below T_g. However, it is found that unlike ordinary spin glasses, the relaxation time of the magnetization at zero field is rather short and the remanent magnetization is negligibly small. These observations indicate that the cluster spin glass state of phase III is a unique state with a short relaxation time at zero field. The numerical calculations using the mean-field approximation indicate that the percentage of partially disordered states is about 50%. The existence of cluster spin glass suggests that the crystal has some randomness, but the origin of this randomness is still unknown. To better understand the nature of this interesting spin glass state, it will be important to measure the time dependence of the magnetization and the frequency dependence of the susceptibility in different magnetic fields. We are currently preparing for these experiments. In this paper, we have suggested the coexistence state of AFM and cluster spin glass based on the thermodynamic physical quantities, but further experimental studies are desired to confirm the coexistence state.

ACKNOWLEDGMENTS

The authors thank T. Oyanagi and M. Wansawa for their help in this research. This work was supported by JSPS KAKENHI Grants No. JP18K03508 and No. JP21K03443.

[1] P. Coleman and A. H. Nevidomskyy, J. Low Temp. Phys. **161**, 182 (2010).
[2] K. Fushiya, T. D. Matsuda, R. Higashinaka, K. Akiyama, and Y. Aoki, J. Phys. Soc. Jpn. **83**, 113708 (2014).
[3] T. Sakakibara, H. Mitamura, T. Tayama, and H. Amitsuka, Jpn. J. Appl. Phys. **33**, 5067 (1994).
[4] J. C. Phillips, Rep. Prog. Phys. **59**, 1133 (1996).
[5] A. P. Ramirez, G. P. Espinosa, and A. S. Cooper, Phys. Rev. Lett. **64**, 2070 (1990).
[6] A. Lacerda, A. de Visser, P. Haen, P. Lejay, and J. Flouquet, Phys. Rev. B **40**, 8759 (1989).
[7] A. de Visser, U. Wyder, D. Schmitt, and M. Zerguine, J. Magn. Magn. Mater. **108**, 59 (1992).
[8] K. Watanabe, H. Kawamura, H. Nakano, and T. Sakai, J. Phys. Soc. Jpn. **83**, 34714 (2014).
[9] S. Nagata, P. H. Keesom, and H. R. Harrison, Phys. Rev. B **19**, 1633 (1979).
[10] H. Yoshizawa, S. Mitsuda, H. Aruga, and A. Ito, J. Phys. Soc. Jpn. **58**, 1416 (1989).
[11] P.-z. Wong, S. von Molnar, T. T. M. Palstra, J. A. Mydosh, H. Yoshizawa, S. M. Shapiro, and A. Ito, Phys. Rev. Lett. **55**, 2043 (1985).
[12] T. Tayama, K. Tenya, H. Amitsuka, T. Sakakibara, A. Ochiai, and T. Suzuki, J. Phys. Soc. Jpn. **65**, 3467 (1996).
[13] K. Fushiya, T. D. Matsuda, R. Higashinaka, and Y. Aoki, Phys. Procedia **75**, 77 (2015).
[14] T. D. Matsuda, R. Higashinaka, and Y. Aoki (Private Communication).
[15] L. R. Sung, Y. D. Yao, W. H. Lee, and Y. Y. Chen, Jpn. J. Appl. Phys. **40**, L154 (2001).
[16] N. Nakamura, R. Higashinaka, K. Fushiya, R. Tsubota, T. U. Ito, W. Higemoto, A. Nakao, R. Kiyanagi, T. Ohhara, K. Kaneko, T. D. Matsuda, and Y. Aoki, JPS Conf. Proc. **29**, 012009 (2020).